Effects of Solvent Viscosity on Polystyrene Degradation in Transient Elongational Flow

Tuan Q. Nguyen* and Henning H. Kausch

Polymer Laboratory, Swiss Federal Institute of Technology, CH-1007 Lausanne, Switzerland

Received January 4, 1990; Revised Manuscript Received April 23, 1990

ABSTRACT: Transient elongational flow created by forcing a liquid across an abrupt contraction was used to investigate the role of solvent viscosity (η_s) on flow-induced degradation of dilute refractionated polystyrene solutions (2 ppm, $\bar{M}_w = 1.03 \times 10^6$, $\bar{M}_w/\bar{M}_n = 1.017$). The viscosity was varied over 2 decades by changing solvent chemical structure while keeping the temperature within a narrow range from 10 to 43 °C. It was observed that the critical strain rate for chain fracture ($\dot{\epsilon}_f$), related to the molecular stress, showed a remarkably weak dependence on solvent viscosity ($\dot{\epsilon}_f \propto \eta_s^{-0.25}$). This result, unexpected in view of the current theories of chain dynamics, could be understood if each distorted molecular coil acted as a microscopic reactor uncoupled from the surrounding fluid apart from the input of deformation energy. It is proposed that "internal viscosity" forces resulting from intramolecular friction between monomer units provided the predominant mechanism for bond scission. This mode of bond activation, which is proposed for transient elongational flows, should be negligible under quasi-steady-state conditions where chains are highly expanded with a low probability of collisions between polymer segments. The precision of midchain scission, already extremely sharp under Θ-conditions (standard deviation $\sigma = 7\%$), tends to be further improved with the quality of the solvent ($\sigma = 4\%$ in 1-methylnaphthalene).

I. Introduction

Long-chain polymers are known to be highly susceptible to degradation by the application of mechanical stress under a variety of experimental conditions.[1] Formation of free radicals by rupture of mechanically stressed chemical bonds has been detected for practically any state of aggregation investigated, whether in amorphous glasses, crystalline solids, rubbery states, melts, or solutions.

Recent efforts have been focused on the degradation in solution, not only because of the technical importance of dissolved polymers (for flow modifications like drag reduction, as viscosity enhancers or antimisting agents) but also because of some definite experimental and theoretical advantages offered by the dilute state:

(1) The low viscosity of a dilute solution allows us to attain the high range of strain rate required for chain scission without excessive viscous heating, which plagued most of the experiments in the solid state.

(2) It is possible to change at will the degree of intermolecular interactions, which either could be short-range electronic forces or could have topological origins like chain entanglements, just by changing the polymer concentration. Intramolecular interactions could also be altered to a large extent by a proper selection of the solvent quality.

(3) Degradation experiments could be carried out under well-defined shear fields by control of the flow geometry. There are essentially two classes of flow fields that are of interest for degradation studies: (a) simple shear field[2] and (b) elongational field.[3]

As far as mechanisms and kinetics are concerned, degradation in simple shear flow is sufficiently distinct from degradation in elongational flow to make it a separate field of investigation. On the basis of recent experimental results, a further subdivision could be made between quasi-steady-state elongational flows, which possess a stagnation point, and transient elongational flows, where the residence time is limited over all streamlines.

When highly dilute polymer solutions where all macromolecules are effectively isolated from each other are used, it is possible to study the degradation behavior of a single chain in flow: the existence of a critical strain rate ($\dot{\epsilon}_f$), below which no chain fracture could occur, was confirmed.[4,5] It was also observed that $\dot{\epsilon}_f$ decreased with increasing molecular weight, in accord with the previous experiments. The determined scaling laws were found to be quite different, however, depending on whether the degradation was performed in an elongational flow created between opposed jets or in sudden acceleration flow (across a narrow contraction); in the former case, a dependence of $\dot{\epsilon}_f$ on M^{-2} was predicted and measured,[3] whereas a lower scaling exponent, $\dot{\epsilon}_f \propto M^{-1}$, had been recorded under transient conditions.[6]

In elongational flows that possess a stagnation point like in the opposed jets device, linear flexible chains could be fully stretched, and they are fractured in this highly expanded state.[3] Such a complete chain orientation could only occur under rather stringent conditions of flow, namely (a) the flow must be "persistently" extensional,[7] (b) the fluid strain rate, $\dot{\epsilon}$, must exceed a critical value $\dot{\epsilon}_{cs}$ for the coil–stretch transition, which is of the order of $0.5/\tau_z$,[3] where τ_z is the longest relaxation time of the chain,[8] and (c) the residence time at the required strain rate $\dot{\epsilon} \geq \dot{\epsilon}_{cs}$ must be much greater than τ_z.[3,9]

Chain degradation in flow is a frequent phenomenon, which could be observed in turbulent flow, which accompanied drag reduction studies,[10] in tube flow at high Reynolds number,[10,11] during melt extrusion,[12] ultrasonic degradation,[13] and gel permeation analysis,[14] or in simple shear flow.[2] In most of these systems, the residence time in the high strain rate zone was too short to meet the last of the above requirements for chain extension, and it is believed that bond scission should take place in a predominantly coiled state. Convergent flow, with its inherent transient residence time, should provide a better representation of the degradation behavior under practical situations of flow than steady-state elongational flow.

Polymer degradations initiated by mechanical forces, known as mechanochemical reactions, are chemical processes in which the activation energy was provided by the input of mechanical stress.[15,16] According to the transition-state theory, the effect of the applied stress was to reduce the activation barrier for bond scission, which

0024-9297/90/2223-5137$02.50/0 © 1990 American Chemical Society

could then be overcome by thermal energy. On the basis of empirical observations, Zhurkov[15] postulated that the rate of chain scission should follow a modified Arrhenius equation:

$$k_c = A \exp[-[(U_0 - f(\psi))/RT]] \quad (1)$$

More recently, a modified version of eq 1 has been derived from the theory of thermal activation barrier for chain scission (TABS).[17]

The kinetic parameters contained in eq 1 are the bond dissociation energy U_0, the elastic potential energy $f(\psi)$, which depends on the acting molecular stress ψ, and the absolute temperature T. As for any thermal activation process, it is expected that the rate of chain scission, k_c, increases with temperature. Experimentally, however, it is repeatedly observed that the rate of shear degradation was the highest at low temperature;[5,18] this constatation was universal to the point that a negative temperature coefficient was considered to be a prime criterion for mechanochemical degradation.[18] The reason for this apparent negative activation energy should be sought in the indirect action of temperature, which, in addition to increasing the probability of fracture of the stressed bond, promotes at the same time the mobility of the chain and of the surrounding medium and lowers the rate of energy input, i.e., the frictional forces at a given shear rate, by this combined effect.

Polymers respond to the application of stress by chain orientation, disentanglement, and bond rupture. Notwithstanding the fact that the relative importance of each mechanism changes with the state of aggregation, structure, and molecular weight of the polymer, the extent of degradation is dependent on the efficiency of transforming the force applied macroscopically into stress at the molecular level. In a few circumstances, stress could be transmitted by external coupling with an electromagnetic field like, for instance, during electrophoresis. By far the most common way of stress transmission, however, was by the mediation of short-range interactions between submolecular entities. In concentrated solutions or in the condensed state, interactions between polymer molecules are additionally effective through the existence of entanglements that act as load-bearing units. In the highly dilute state where each macromolecule is isolated from the other, stress is transmitted by inelastic exchange of momentum between polymer segments and flowing solvent molecules; when a velocity gradient is present, dissymmetry of the Brownian motion between portions of the same macromolecule gives rise to molecular tensions leading to a change in chain conformation and, ultimately, to bond rupture. In most of the current theories of chain dynamics in solution, the frictional contact between polymer segments and solvent molecules, known as the "monomer–solvent friction coefficient" (ζ), is assumed to be directly proportional to the bulk viscosity of the solvent. Solvent viscosity, thus, plays an active role in channeling part of the kinetic energy of the flow into the bond potential energy; in this respect, it should stand on the same foot as strain rate and molecular weight as one of the fundamental parameters that control the kinetics of degradation in flow.

In a few studies,[5,19] solvent viscosity was varied as a result of change in temperature. Since both η_s and T affect the degradation kinetics, it is desirable to look for a system where each factor could be studied independently. In the present investigation, we try to separate the two effects by looking at a system where the solution viscosity could be varied over the broadest range, while keeping at the same time the solvation power and temperature within the narrowest possible limits.

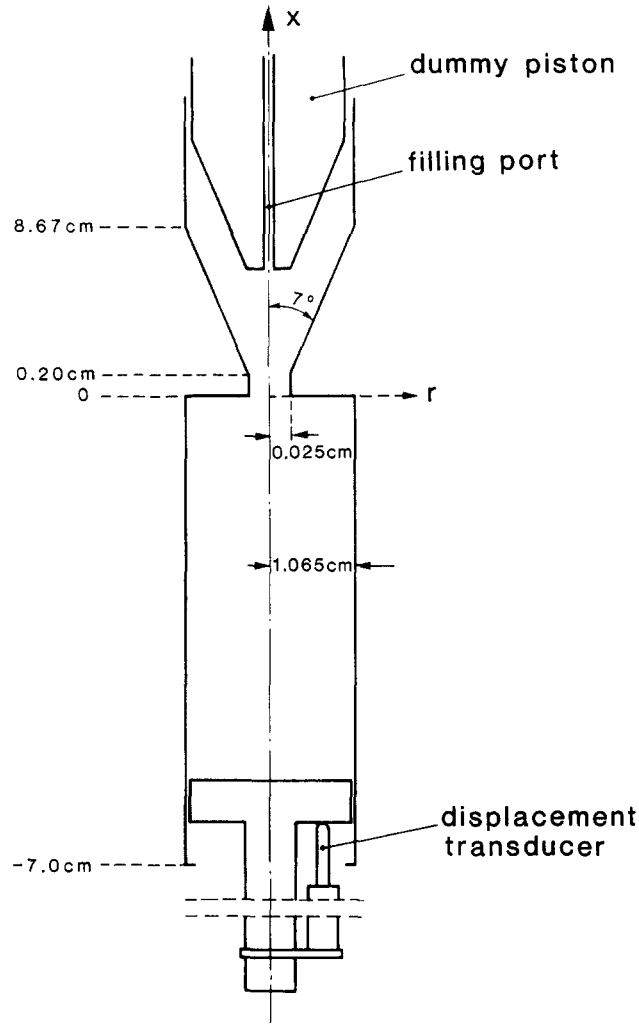

Figure 1. Schematic representation of the degradation apparatus (dimensions are not drawn to scale).

II. Experimental Section

Degradation Apparatus. The degradation equipment was the same as used previously[5,20] and is schematically described in Figure 1. It consists of a stainless steel syringe thermostated with a water jacket. The polymer solution, confined to the lower reservoir, was pushed at constant speed across the orifice by means of a pneumatic actuating cylinder. The sudden acceleration of the fluid across the contraction creates a flow field of high strain rate ($\dot{\epsilon}$) with a residence time as short as a few microseconds. The velocity of the piston, monitored by a displacement transducer, was shown to be constant to better than 2% over the complete 7-cm course. The highest strain rate attainable is determined by the force applied on the piston and by the solution density; in methyl acetate, a maximum value of $\dot{\epsilon} = 8 \times 10^5\ s^{-1}$ was obtained when the pressure inside the reservoir compartment reached 200 bar.

Chemicals. Polystyrene samples are standards from Polymer Laboratories; they are refractionated on analytical GPC columns to reach the extreme low polydispersity required for the experiments.

All the solvents are of the purest grade available from Fluka AG and are distilled prior to utilization.

Decalin is a commercial mixture containing 41% *cis*-decahydronaphthalene + 58% *trans*-decahydronaphthalene + 1% tetrahydronaphthalene as determined by gas chromatography.

Molecular Weight Determination. Molecular weight distributions of virgin and degraded polymer solutions are determined by gel permeation chromatography (GPC) on a Waters

150C equipped with a variable-wavelength UV detector (Perkin-Elmer 75C) and modified to allow data acquisition and processing with a personal computer (Hewlett Packard 9816). A set of Ultrastyragel columns ($2 \times 10^6 + 1 \times 10^5$ Å) was used for the separation. All the data are corrected for instrumental dispersion.

Degradation Conditions. Only single-passage degradation is used for the experiments. Dissolved oxygen is known to be an efficient radical scavenger;[2] to avoid secondary reactions from macroradicals formed during the degradation, solutions are saturated with air prior to the experiment.

Highly dilute solutions containing 2 ppm of polymer are used for the degradation, this choice was dictated by practical and theoretical considerations:

(1) The quantity of refractionated material was limited and should be used efficiently. Each experiment necessitated 25 mL of solution, which is equivalent to 0.05 mg of polymer: this amount is amply sufficient for GPC measurement due to the high UV absorption coefficient of polystyrene at 252 nm.

(2) Under shear flow, macromolecular coils are expanded and the limit of intermolecular interactions is much lower than under quiescent conditions. The use of low polymer concentration ensures that the molecular coils are effectively isolated from each other.

(3) Viscoelasticity is the very essence of polymeric liquids. Flow modelization of viscoelastic fluids is complex since it requires the knowledge of the nonlinear relationship between stress and deformation, which enter into the constitutive equation. Fortunately, viscoelasticity is concentration dependent;[21] working at high dilution could relieve much of this complication. At the present range of molecular weight and concentration, the solution should behave approximately as a Newtonian fluid, whose flow properties are described by the Navier–Stokes equations.

Viscosity Measurements. The kinetic viscosity of solvents and polymer solutions was determined with an automatic Ubbelohde viscometer (Schott Model AVS-100). Intrinsic viscosity was obtained by linear extrapolation from measurements at three different concentrations. The solvent density used to convert kinetic viscosity into absolute viscosity was measured with a calibrated Bingham picnometer.

Determination of Θ-Temperature. The Θ-temperature of PS in the different solvents was determined by the phase equilibria method; the maximum of the cloud-point curve was extrapolated to infinite molecular weight according to the Schulz–Flory plot.[22] Data reported in the literature show a linear decrease of the Θ-temperature with the content of cis isomer in decalin;[23] the value extrapolated to the present composition is in perfect accord with the experimental temperature of 14.8 °C.

III. Results

Solvent Selection. The scaling laws for $\dot{\epsilon}_{cs}$[6] and for molecular properties of the polymer are well-established under Θ-conditions. To benefit from these results and in order to keep the number of parameters at a minimum, we will try to work as closely as possible to the Θ-conditions.

The solvents are selected according to the following criteria:

(a) They should have a convenient Θ-temperature easily accessible to experimentation.

(b) The viscosity should cover the largest possible range.

(c) To recover the polymer for GPC analysis, the solvent should have a sufficiently low boiling point to allow its complete removal by vaccum distillation without thermal degradation of the solute.

This last constraint excludes the use of bis(2-ethylhexyl) phthalate (DOP) as a solvent, although this compound combines two desirable features for the present investigation, i.e., a $T(\Theta)$ near room temperature and a high bulk viscosity (cf. Table I).

Amongst the other aliphatic phthalic esters that had been tested, only dimethyl phthalate could be quantitatively removed by vacuum distillation at $T < 120$ °C. This ester remains a good solvent for PS at low temperature, and no cloud point was detected even at −20 °C.

Table I
Physical Constants of Some Selected Solvents for PS

solvent	η_s,[a] mPa·s	ρ,[a] g·cm^{-3}	T,[b] °C	bp,[c] °C
methyl acetate	0.329	0.902	43.5 (Θ)	57
cyclohexane	0.772	0.765	34.5 (Θ)	81
decalin	2.769	0.890	14.8 (Θ)	189–191
1-methylnaphthalene	2.793	1.014	27.0	241–245
dimethyl phthalate	32.10	1.200	10.0	283–288
DOP	65.00	0.985	22.0 (Θ)	386
didecyl phthalate	10.46	0.918	72.5 (Θ)	

[a] η_s and ρ are measured at the temperature given in column 4. [b] The index Θ indicates the Θ-temperature. [c] Boiling point at atmospheric pressure, as given in the literature.

In view of the size of the molecular coil (Table II) and of the small second virial coefficient (A_2) observed in this solvent, it seems that the determined value of 0.87 for the exponent a in the Mark–Houwink equation is abnormally high for some unclear reasons.

To determine the influence of solvent quality on the degradation kinetics, some comparative experiments are performed in a good solvent (1-methylnaphthalene) and in a Θ-solvent (decalin) at temperatures where the two solution viscosities perfectly match each other (Table I).

Two important molecular quantities relevant to chain hydrodynamics could be obtained from the intrinsic viscosity, namely, the terminal relaxation time (τ_z) to be discussed in section IV and the coil hydrodynamic radius (R_h).

From Table II, it could be verified that the macromolecular coils are more expanded in a good solvent like 1-methylnaphthalene than in the poor solvents. At a given solvent viscosity, the more expanded coil has also a longer relaxation time, which means that it started to be deformed at a lower strain rate of the surrounding fluid.

Flow Field Analysis. Kinetics of polymer degradation is sensitive to subtle modification of chain conformation, which in turn depended on the details of the pervading flow field.[25] Hence, special care should be given in the design of the exit nozzle and on flow field calculations to ensure meaningful interpretation of the results.

In the present work, we used extensively the finite element program POLYFLOW[26] for flow field calculations and as a computer-assisted tool for the proper design of the exit nozzle. This flow modeling program is capable of handling steady-state and time-dependent laminar flows of both Newtonian and viscoelastic fluids. The only requirement, that of fluid incompressibility, is easily satisfied in the present context.

A simplification was introduced in previous flow field computations by considering that inertial forces dominated the flow and neglecting viscous forces (inviscid approximation). Since solvent viscosity is now systematically varied over large limits, the above approximation may be not be valid over the whole range and viscous forces are explicitly considered in the flow equations. Results of computations showed, nevertheless, that, even with bis(2-ethylhexyl) phthalate (η_s = 65 mPa·s), viscous forces did not affect the flow field until fluid velocities dropped below 0.2 m·s^{-1} at the orifice; this is 2 orders of magnitude lower than the actual range used in the present investigation.

The flow geometry is time-dependent with the constant advance of the piston during the experiment. The flow field, however, was not significantly perturbed by this displacement except when the plunger reached a few millimeters before the end of its course. The spatially steady-state flow hypothesis is thus a good approximation; to further improve the constancy of the flow field, a collar

Table II
Molecular Properties of Polystyrene in the Different Solvents

solvent	τ_z, μs	ϵ_f^*, 10^5 s^{-1}	$[\eta]$, dL·g^{-1}	K, dL·g^{-1}	a	R_g, nm	λ(fluid)	σ
methyl acetate	8	3.48	0.737	72×10^{-5}	0.50	26.1	2.1	0.08
cyclohexane	23	2.84	0.863	85×10^{-5}	0.50	27.6	5.3	0.07
decalin	82	2.06	0.812	80×10^{-5}	0.50	27.0	7.1	0.07
1-methylnaphthalene	240	2.06	2.44	87×10^{-6}	0.74	39.0	15.3	0.04
dimethyl phthalate	1400	0.92	1.14	67×10^{-7}	0.87	30.2	31.4	0.06
dimethyl phthalate[a]	9200	0.25	2.77	67×10^{-7}	0.87	40.6	37.7	0.11
dimethyl phthalate[b]			1.17	67×10^{-7}	0.87			

[a] Polystyrene with $M = 2.86 \times 10^6$, $\bar{M}_w/\bar{M}_n = 1.02$. [b] Measured at $T = 25$ °C.

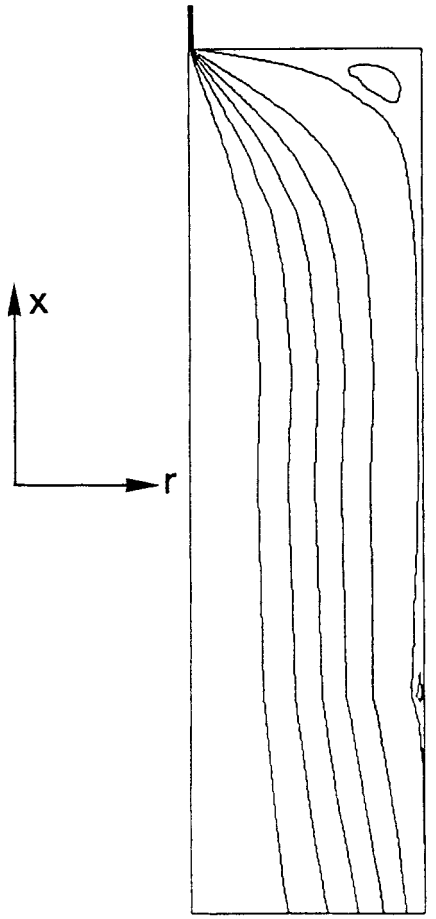

Figure 2. Streamlines computed for a midtravel distance of the piston at $x = -4.0$ cm (the position of the orifice is taken as the origin). Due to axial symmetry, only half of the flow tube is shown.

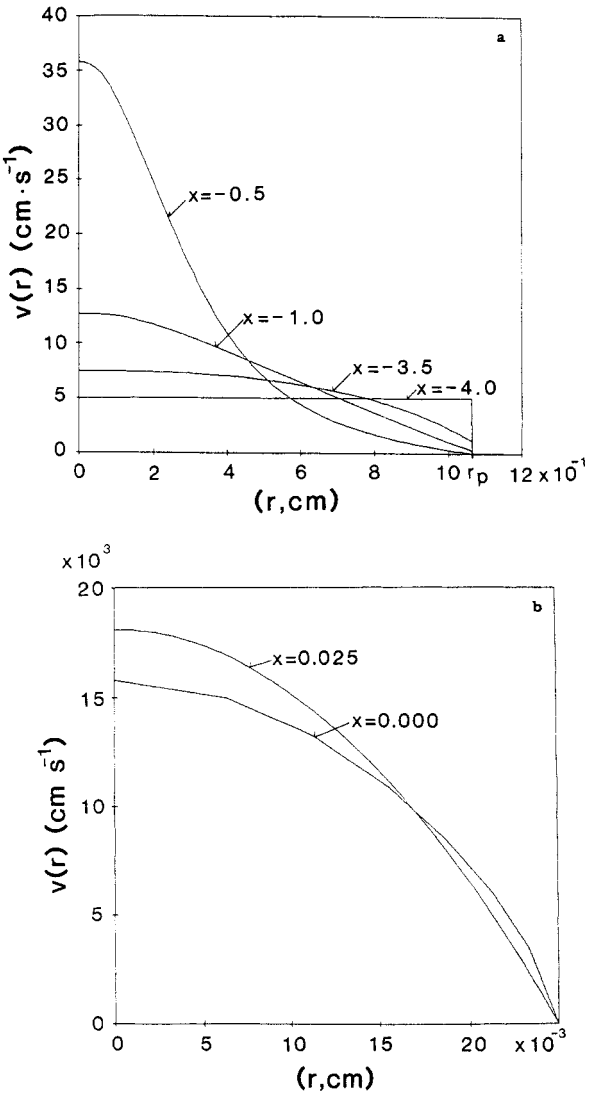

Figure 3. Axial distribution of the fluid velocity calculated at different distances from the orifice (the piston was moving with a speed $v_p = 5$ cm·s^{-1}): (a) before the orifice; (b) in the vicinity of the orifice.

was added in a later design to stop the piston movement 0.6 cm before touching the orifice.

Flow field calculations are conveniently performed in dimensionless parameters. To give a better visualization of the flow, we intentionally give the results with their real physical units. The streamlines calculated for different values of the stream function are shown in Figure 2. Some flow recirculation is visible around the corners, but this is negligible as compared to the viscoelastic situation. The velocity profiles, calculated for different distances from the orifice at a midtravel distance of the piston, are shown in parts a and b of Figure 3.

The computed velocity field has several distinctive features associated with a transient elongational flow:

(1) Most of the fluid acceleration occurred within ~1 orifice radius ($r_0 = 0.025$ cm) in front of the convergent inlet. This sudden acceleration is reflected in the impulselike shape of the strain rate (Figure 4a), which can reach extremely high amplitudes but only over a limited region of space. The residence time of a fluid element entering the region of high strain rate, along any streamline, is typically on the order of 2–10 μs under present flow conditions: converging flows are termed "transient" flow due to this short residence time.

(2) Although most of the fluid acceleration occurred before the inlet, the velocity distribution reached a steady value only after traveling some distance inside the capillary section (Figure 3b).

At this stage the velocity distribution showed the typical parabolic shape characteristic of a fully developed velocity profile. The flow field could be significantly perturbed by the downstream region, and it is thus important to keep a short straight distance after the orifice (Figure 1), long

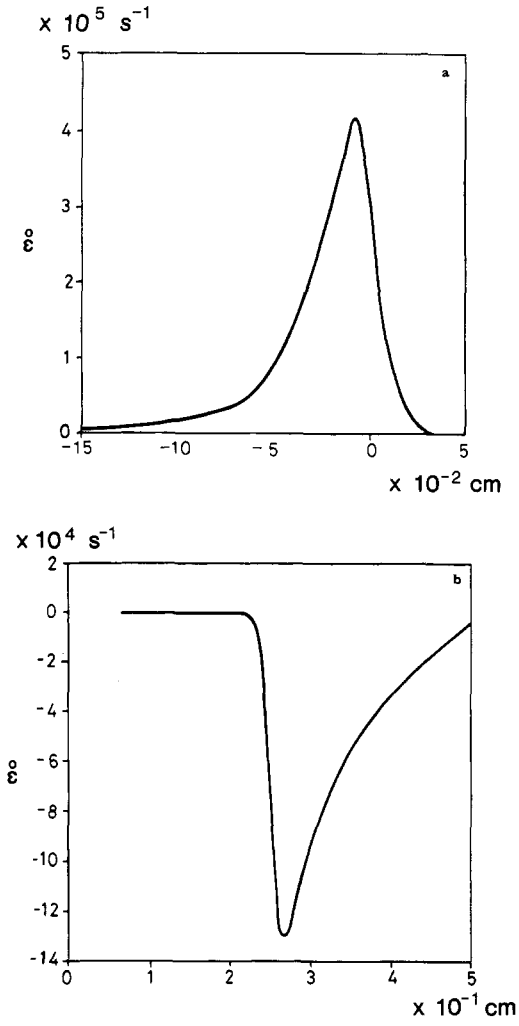

Figure 4. Elongational strain rate ($\dot{\epsilon}_{xx}$) calculated along the center line of the flow tube with v_p = 5 cm·s^{-1}: (a) convengent flow before the orifice; (b) divergent flow after the orifice (14° conical outlet). ($\dot{\epsilon}_{xx} = \partial v_x/\partial_x$, v_x = velocity component along the flow direction.)

enough for the velocity to reach a steady value but at the same time sufficiently short to avoid shear degradation induced by the high velocity gradient present next to the capillary walls.

(3) With incompressible liquids, the volumetric average velocity at the orifice ($\bar{v}_0$) is given by

$$\bar{v}_0 = v_p(r_p/r_0)^2 \qquad (2)$$

where r_p is the piston radius (1.065 cm).

From the parabolic distribution of the velocity front, the maximum velocity at the symmetry axis $v_0(o)$ is twice the average velocity $\bar{v}_0$. As a consequence, the maximum strain rate along the center line (Figure 4a) is also a factor of 2 larger than the values calculated with reference to $\bar{v}_0$ and that are reported in previous publications.[5,20,27]

(4) As with any elongational flow, the velocity field is not homogeneous. Flow is purely elongational only along the central streamline and becomes simple shear next to the walls. Flow remained "strong", however, for a large part of the tube, and a kinetics study taking this variation of strain rate into account was recently presented;[25] the influence of orifice diameter on flow field characteristics is under current investigation.[28]

(5) The divergent outlet was used to avoid backflow convection and excessive shear buildup after the contraction. As a result of the deceleration flow, the fluid element experienced a uniaxial compression shown as negative strain rates in Figure 4b. With the 14° conical outlet in the present design, the amplitude of the negative strain rates attains as much as one-third of the maximum value of the extensional strain rate. In a few experiments, we either removed the conical outlet to allow the outcoming jet to exit freely into a collecting reservoir or replaced the 14° conical section with a 5° tapered outlet (thus reducing the range of negative strain rates by a factor of 8). In each case, analyses did not show any significant change in the scission yield as compared to the standard design, which tends to confirm that most of the degradation took place in the elongation flow region before the orifice and not as a result of biaxial extension or turbulences in the downstream section.

Accumulated Strain. The total strain accumulated by a fluid element flowing along the centerline is given by the ratio

$$v_0(o)/v_p \sim 2(r_p/r_0)^2 = 3630 \qquad (3)$$

The extension ratio of a polymer molecule embedded in the fluid element is, however, much less than the corresponding strain for two reasons:

From a theoretical basis, it is believed that the molecular coil starts to deform only near the critical strain rate for the coil–stretch transition ($\dot{\epsilon}_{cs}$) and progressively recovers its initial conformation at lower values of $\dot{\epsilon}$(fluid). In case of an affine deformation, the upper limit to the degree of coil extension is given by the total fluid strain accumulated within the spatial region, where $\dot{\epsilon}$(fluid) $\geq \dot{\epsilon}_{cs}$. This quantity, denoted by λ(fluid), is reported in Table II. Large incertitude exists in the correct value to be used for $\dot{\epsilon}_{cs}$. The experimental results reported by Bristol's group in opposed jets[29] are significantly higher (by a factor of 3–5) than the values obtained from the condition $\dot{\epsilon}_{cs}\tau_z \sim 0.5$ (eq 4). In Table II, we refer to these experimentally determined values, extrapolated to the actual molecular weight and solvent viscosities, to calculate λ(fluid).

The unperturbed end-to-end distance (R_0) of a flexible polymer chain is equal to 67 nm for a 10^6 $\bar{M}_w$ polystyrene.

Since the maximum extended length (l_{max}) of the same chain is 2500 nm, it can be assessed that the coil will never reach a state of full chain extension if λ(fluid) < l_{max}/R_0 ~ 37 (Table II).

When the preceding reasoning is used, the effective residence time (τ_r) of the chain could be calculated as the time spent by the molecule to cross the region of "strong" flow, which satisfies the above-mentioned strain rate conditions: this turns out to be $<\tau_z$ for most solvents under consideration.

Degradation Results. After a single passage across the orifice above the critical strain rate ($\dot{\epsilon}_f$), an increasing proportion of dissolved polymer molecules was degraded with a sharp propensity for midchain scission. At sufficiently high strain rate, macromolecules that have experienced two successive scission events could eventually be observed on the GPC traces at one-fourth of the initial molecular weight (Figure 5).[5,25] The details of the data treatment and kinetics analysis have been described elsewhere[6,25] and consist of the following steps:

(1) The detector output from the chromatograph is corrected for instrumental dispersion, using one of the techniques currently available.[30,31]

(2) The ratio of the degraded peak to the total surface under the GPC trace gives the scission yield, which is the weight fraction of polymer that has been degraded. Reporting the scission yield as a function of strain rate

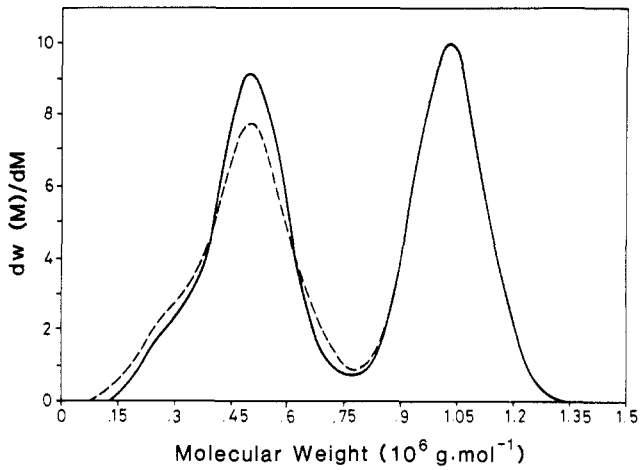

Figure 5. Molecular weight distribution of a polystyrene sample ($\bar{M}_w$ = 1.03 × 10^6, $\bar{M}_w/\bar{M}_n$ = 1.017) after degradation in decalin (—) and in 1-methylnaphthalene (- - -). The data have been corrected for instrumental broadening.

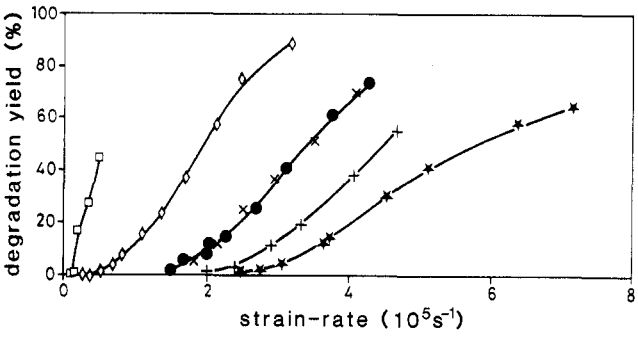

Figure 6. Degradation yield as a function of strain rate, $\dot{\epsilon}(0)$, and solvent viscosity ($\dot{\epsilon}(0)$, maximum elongational strain rate along the center line). Excepted for the first series, all the data refer to the same PS fraction sample with $\bar{M}_w$ = 1.03 × 10^6, $\bar{M}_w/\bar{M}_n$ = 1.017: (-□-) dimethyl phthalate ($\bar{M}_w$ = 2.86 × 10^6, $\bar{M}_w/\bar{M}_n$ = 1.02); (-◇-) dimethyl phthalate (η_s = 32.1 mPa·s); (-●-) decalin (η_s = 2.77 mPa·s); (-×-) 1-methylnaphthalene (η_s = 2.79 mPa·s); (-+-) cyclohexane (η_s = 0.772 mPa·s); (-★-) methyl acetate (η_s = 0.329 mPa·s).

allows us to localize the critical strain rate $\dot{\epsilon}_f$, which marks the onset for chain scission (Figure 6).

(3) Polydispersity is an unavoidable complication when working with synthetic polymers. An anionic PS standard with a polydispersity of 1.05 and a Schulz–Zimm distribution cover practically a decade range of molecular masses. Even the refractionated sample with $\bar{M}_w/\bar{M}_n$ = 1.017 still contained macromolecules encompassing a factor of 2 in chain length.

Since the rate of mechanochemical degradation strongly depends on the molecular chain length, it could be realized that molecular weight distribution has a decisive influence on the experimental results and should be properly taken into account for meaningful evaluation of the kinetic parameters. To give the best accuracy, it is always desirable to work with samples having the lowest polydispersity available. The shape of the degradation yield curve results from the cumulative effects of polydispersity and strain rate distribution across the degradation tube (cf. section III, Flow Field Analysis). As discussed in more detail previously,[25] the experimental $\dot{\epsilon}_f$ refers to the highest molecular weight present in the undegraded sample. In order to obtain the effective $\dot{\epsilon}_f$* related to one specific molecular weight (for example, molecular weight at peak maximum, $\bar{M}_w$, $\bar{M}_n$, etc.), some proper kinetics analysis should be performed, taking into account both the molecular weight distribution of the starting material and

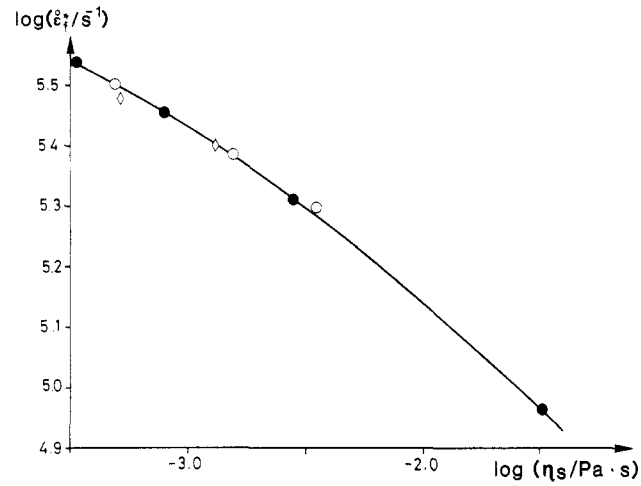

Figure 7. Dependence of the critical strain rate for chain scission ($\dot{\epsilon}_f$*) on solvent viscosity (η_s). (-●-) Data from this work. Previous data from ref 5, where $\dot{\epsilon}_f$ was changed concomitantly with the solvent temperature: (-○-) decalin at 7, 22, and 140 °C; (-◇-) dioxane at 22 and 90 °C.

the scaling law between $\dot{\epsilon}_f$ and M. In the present case, the values of $\dot{\epsilon}_f$* reported in Table II refer to the weight-average molecular weight of the sample ($\bar{M}_w$) and correspond to a degradation yield of ~10% on the degradation curves.

In the present experiment, the prime variable is solution viscosity. However, since the polymer content is extremely low, it is practically equal to the pure solvent viscosity. Plotting $\dot{\epsilon}_f$* as a function of η_s on a double-logarithmic scale gives a smooth curve with an average slope of −0.25 (Figure 7), far below from the expected value of −1.0 if a reciprocal proportionality existed between $\dot{\epsilon}_f$* and η_s.

The location of the scission point on the backbone is a quantity of great interest, capable of providing significant insight into the mechanism of coil extension and fracture. On the basis of a matrix technique developed for first-order depolymerization kinetics,[13] the probability of scission along the chain could be determined by a curve-fitting procedure.[13,25] Generally, it was found that the probability of bond scission along the chain could be described by a Gaussian distribution function with a standard deviation σ, which characterizes the sharpness of the chain-halving process.[2,25] It was found previously that the parameter σ increased slightly with the molecular weight but was independent of the degradation yield. The values for σ calculated according to the above-mentioned method and reported in Table II refer to a scission yield of ca. 50%. With the exception of 1-methylnaphthalene, all the determined σ are comparable to those obtained previously in decalin.[6]

Effect of Degradation Temperature. To keep the solvent quality close to the Θ-conditions, we have changed the temperature from 10 to 43.5 °C. From the form of eq 1, it is intuitively expected that the rate of chain scission (k_c) and consequently $\dot{\epsilon}_f$ should be strongly dependent on temperature. Detailed kinetic analysis, disregarding the effect of change in solvent viscosity, demonstrated on the contrary that $\dot{\epsilon}_f$ was lowered by as little as 6–7% when the degradation temperature increased from 7 to 140 °C.[5] This remarkable result is a consequence of the spikelike shape of the strain rate distribution (Figure 4a) and is applicable exclusively to the transient flow situation. A "normal" Arrhenius-type dependence of $\dot{\epsilon}_f$ on temperature was actually observed under stagnant elongational flow.[19]

We have reported in Figure 7 some previous results on $\dot{\epsilon}_f$ measured in decalin and in dioxane as a function of

temperature.[5] Notwithstanding the larger range of temperature that has been covered, the ancient data points follow closely on the same curve as the recent values: this tends to support the idea that temperature and solvent quality have little influence on the mechanochemical degradation in transient elongational flow.

Effect of Molecular Weight and Residence Time. In relation to the relaxation time (τ_z) (eq 4), the effective accumulated strain given by λ(fluid) of a polymer chain near the critical strain rate for chain scission ($\dot{\epsilon}_f^*$) increases with the solvent viscosity and molecular weight (Table II). It is thus expected that long-chain polymers in viscous solvents could achieve a high degree of coil extension before bond rupture in convergent flow, in similarity to the situation observed under quasi-steady-state elongational flow.

Values of $\dot{\epsilon}_f^*$ measured in dimethyl phthalate for two samples with $M = 2.86 \times 10^6$ and $M = 1.03 \times 10^6$ showed a dependence on $M^{-1.3}$, a significant departure from the M^{-1} scaling law, which is thought to be characteristic of the degradation behavior of partly uncoiled polymer chains, but still far from the M^{-2} law observed for highly extended chains. Presumably, some intramolecular mechanism prevented the coil from following an affine deformation with the surrounding fluid even if $\dot{\epsilon} > \dot{\epsilon}_{cs}$.

IV. Discussion

The most outstanding feature revealed by the experimental data reported in Figure 6 and Table II is the relative insensitivity of $\dot{\epsilon}_f$ to a large change in solvent viscosity: increasing η_s by 2 orders of magnitude in going from methyl acetate to dimethyl phthalate merely reduced $\dot{\epsilon}_f^*$ by a factor of 3.4. This weak dependence of $\dot{\epsilon}_f^*$ on η_s, already noticed but left unexplained in a previous work on the effects of temperature,[5] is unexpected from current theories of chain dynamics, which assume a proportionality between the molecular stress and solvent viscosity.

Chain unraveling and fracture in flow are highly complex processes and their modeling is still in an evolving phase of development.

Prestretched State. Using the dumbbell model with a single time constant for a linear flexible polymer chain, de Gennes predicted a sharp coil-to-stretch transition at $\dot{\epsilon}\tau_z \sim 0.5$,[32] where τ_z is Zimm's relaxation time given by[8]

$$\tau_z = M_{\eta_s}[\eta]/1.18RT \tag{4}$$

The above result is supported by a number of experiments,[3,33] in particular by birefringence measurements in stagnant elongational flow.[3,34] When the partly uncoiled polymer chain is modeled as an impenetrable cylinder of length L and diameter d, oriented along the flow direction, the stress acting along the chain was evaluated by using the results of slender-body hydrodynamics:

$$F_{max}(\text{center}) = [(2\pi/\ln(L/d)]\eta_s\dot{\epsilon}L^2/8 \tag{5}$$

Results on degradation obtained between opposed jets also amply confirmed the dependence of the critical strain rate for chain fracture ($\dot{\epsilon}_f$) on the molecular weight and on solvent viscosity[4] as predicted by eq 5:

$$\dot{\epsilon}_f \propto \eta_s^{-1}M^{-2} \tag{6}$$

Recent numerical simulation[35,36] and experimental results[37,38] showed that the deformation in extension of a flexible polymer chain is far more complex than suggested by the single coil–stretch transition for the entire molecule: the local and overall extension of the coil evolve over different time scales. Deformation of the molecular coil starts at short times with lateral contraction; at much longer times, the distances between each bead extend nearly uniformly up to the maximum before appreciable unraveling could occur. In the long time limit, calculations tend to confirm the existence of a coil–stretch transition (although not as sudden as suggested by the de Gennes picture), with the exact value of $\dot{\epsilon}_{cs}$ changing somewhat according to the model.[35,36]

From the above considerations, it is expected that the chain in transient elongational flow does not have sufficient time to unravel to an appreciable extent during the short transit time in the extensional region and retains a partially coiled conformation up to the scission.

On the basis of the slender-body hydrodynamics (eq 5), it has been proposed[39] that the maximum acting stress, and, hence, the critical stress for chain fracture ($\dot{\epsilon}_f$) of a partly uncoiled polymer, should scale like the root-mean-square radius of gyration of the macromolecule, which is proportional to molecular weight under Θ-conditions:

$$1/\dot{\epsilon}_f \propto R_g^2 \propto M \tag{7}$$

Although the proposed scaling law seems to conform to the experimental results,[6] the slender-body hydrodynamics model is unsatisfactory in many respects:

(1) As a result of the weaker dependence of $\dot{\epsilon}_f$ on M in transient elongational flow ($\dot{\epsilon}_f \propto M^{-1}$ vs $\dot{\epsilon}_f \propto M^{-2}$ under stagnant conditions), scission will occur at lower strain rates below a certain value of the molecular weight. From experimental data,[3,6] it could be estimated that this crossover molecular weight was $\sim 2 \times 10^6$. This result is in complete contradiction with the hydrodynamic screening concept of non-free-draining coils where the gripping action of the flow increases steeply with the degree of coil expansion.

(2) When eq 5 and the experimental data in cyclohexane are used as an example (Table II), it is possible to evaluate the forces involved during the coil stretching. With $L = 690$ nm, $d = 130$ nm ($\lambda = 5.3$), $\eta_s = 0.772$ mPa·s, and $\dot{\epsilon}_f = 2.84 \times 10^5$ s^{-1}, $F_{max} = 5 \times 10^{-11}$ N. This value is over 2 orders of magnitude below the breaking stress of a C–C bond, which is around 6–8 nN,[40] and, therefore, no bond scission should occur following the proposed model.

(3) From eq 5, a linear relation between $\dot{\epsilon}_f$ and η_s^{-1} is expected, which is nonconsistent with the present results.

(4) The dependence of $\dot{\epsilon}_f$ on R_g^2 implies that the scaling law is dependent on solvent quality, since

$$R_g^2 \propto M^{2\mu} \tag{8}$$

with $\mu = 0.50$ in Θ-solvents, 0.55–0.60 in good solvents,[24] and 0.33 in the collapsed state.[41]

Since R_g^2 and τ_z are much larger in 1-methylnaphthalene than in decalin (Table II), it is expected that the coil should also start to deform and then break at a lower critical strain rate. The experimental data tend to confirm otherwise: the degradation curves in methylnaphthalene and in decalin are exactly superposable under conditions of viscosity matching, which may signify that only the viscosity, and not the quality of the solvent, has an influence on the fate of the degradation process. Whether this concordance was fortuitous or stemmed from deeper origins needs further investigation on a series of samples with different molecular weights.

(5) The slender-body model does not explain the precise midchain scission that is invariably observed (Figure 5). On the basis of the shape of the stress distribution function (eq 5), it was argued that the chain should start to unravel from the center where the tension was the highest. This picture, first proposed by Kuhn[42] and then by Frenkel,[43]

has recently surfaced with the so-called "yo-yo" model to explain coil dynamics under transient flow.[44] This model, which could qualitatively account for the midchain scission, is, nevertheless, challenged by the more recent theoretical and experimental results.[37,45]

Internal Viscosity. The Rouse–Zimm bead–spring is a coarse-grained representation of the large-scale behavior of long flexible chains. The model assumes that the polymer is completely limp except for the elastic spring force to resist stretching; in addition, the impossibility for a physical chain to cross itself is ignored (phantom chain model). To describe the deformation of a real polymer chain, Kuhn[46] recognized that the rotational energy barriers between different local conformations could hinder the extension and contribute to an internal force (F^{iv}), which should be added to correct for the force balance equation. This first model of "internal viscosity" was independent of solvent viscosity but decreases with the polymer chain length.

Subsequently, to explain some rheological data at high shear rate, like the high-frequency dynamic viscosity or the shear thinning of polymer solution, an additional internal viscosity term was proposed by Cerf,[47] which is independent of both solvent viscosity and chain length:

$$F^{iv}(\text{Cerf}) = \zeta\dot{r} \tag{9}$$

In the above equation, ζ is a proportional constant independent of solvent viscosity and $\dot{r}$ is the extension rate of the bead–spring chain.

Internal viscosity is generally considered as a convenient parameter to fit theory with experiments. The real significance of internal viscosity has been frequently questioned, however, because its description is often vague and its quantification cannot be calculated from molecular structure. The most appealing feature of internal viscosity forces in the context of the present work is its independence from solvent viscosity, a fact that bears qualitative resemblance to our degradation results.

In the following section we show, using simple scaling arguments, that internal viscosity, which plays an essential role in polymer rheology, could also explain some of the degradation results in transient elongational flow. The derivation is far from being rigorous and should be taken as a tentative explanation for a new phenomenon that needs further experimental support and theoretical refinement.

In analogy with thermally activated chemical reactions, it is plausible to assume that the rate of bond scission is proportional to the frequency of collisions between a given polymer segment and the surrounding molecules (via the preexponential factor). In transient elongational flow, the chain started to deform from a compact coiled state. The probability of intersegmental friction is nonnegligible and could provide a significant contribution to the mechanism of bond activation. The proposed model is essentially similar to the "large loop" representation put forward by de Gennes[48] to account for the origins of Cerf's internal viscosity (Figure 8).

From the results of chain statistical mechanics, the probability that a monomer unit situated at position m comes into close contact with another unit located at n is given by[49]

$$p_{nm} = A|n - m|^{-\gamma} \tag{10}$$

Depending on the details of the theoretical treatment, the exponent γ falls within the region $1.5 \leq \gamma \leq 2.0$, although $\gamma = 2$ was favored by de Gennes in his treatment, which we will now follow.

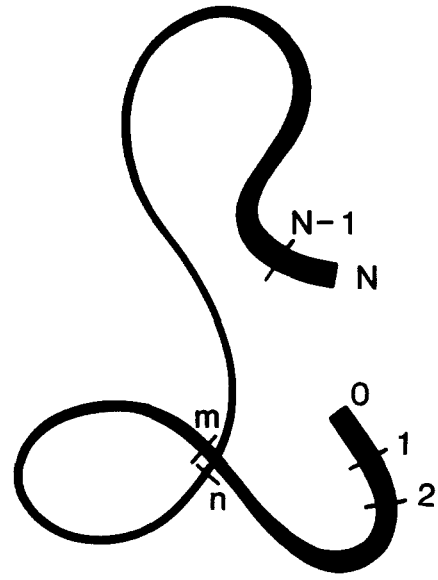

Figure 8. Large-loop model for the origins of internal viscosity (according to de Gennes[48]).

During the deformation, each contact point will contribute to a dissipation of energy equal to

$$\zeta(\dot{r}_n - \dot{r}_m)^2 \tag{11}$$

It was assumed that the chain deforms according to a linear law:

$$\dot{r}_n - \dot{r}_m = (n - m)/N\dot{r} \tag{12}$$

If relation 10, which was derived under the absence of external force, could be extrapolated to the dynamic conditions of flow, the rate of energy dissipated per chain ($T\dot{S}$) as the result of internal viscosity is now obtained by substituting eq 12 into eq 11 and summing over all the monomer units:

$$T\dot{S} = (^1/_2)(\dot{r})^2\zeta N^{-2}\sum_{n,m} p_{nm}(n - m)^2 \tag{13}$$

It turns out that eq 13 is independent of N and is proportional to $(\dot{r})^2$.

Over the coil dimensions, the elongational strain rate, $\dot{\epsilon}$, is practically constant and $\dot{r} \propto \dot{\epsilon}R_g$, giving a rate of energy dissipation proportional to $(\dot{\epsilon}R_g)^2$. Under Θ-conditions, $R_g \propto M^{1/2}$ and the proportionality between $\dot{\epsilon}_f$ and $1/M$ could now be deduced on energetic grounds without having recourse to the slender-body hydrodynamics. The apparent independence of $\dot{\epsilon}_f$ on the solvent quality, if confirmed, could not be explained without some further modification to the model (like for example, the presence of metastable states at intermediate coil expansion prior to scission).

V. Conclusion

Polymer degradation in flow results from a coupling between hydrodynamic, statistical, and quantum mechanical effects. The dynamics of chain uncoiling is slow on a hydrodynamic scale as suggested by theoretical and experimental investigations; the existence of metastable conformations with extended lifetimes during the deformation is nonnegligible. The mechanisms of bond scission, being controlled by the degree of chain extension, evolve with the time scale of observation. Differences in degradation behavior observed under stagnant and under transient elongational flow could be rationalized if each

type of flow probed a different conformation of the chain during the uncoiling stage.

Under quasi-steady-state elongational flow, the chain was allowed sufficient time to reach the fully extended state; if only the equilibrium conformation was monitored as with the birefringence measurements, then a single relaxation time is sufficient to describe the coil-to-stretch transition. At this stage, the highly expanded chain is free-draining and the molecular stress is solely determined by the friction action of the solvent. In transient elongational flow, on the contrary, the sudden deformation of the chain while still in the coiled conformation favors intramolecular contacts, which act as many gripping points for the stress transmission. In the limit, the surrounding solvent molecules serve only as an energy source for the process of coil deformation while intersegmental friction determines the level of acting stress along the chain similar to the deformation in the condensed state. The degradation kinetics should then be more sensitive to alteration of the intersegmental friction coefficient (by changing the polymer chemical structure) than to that of the solvent viscosity, a feature which needs further experimentation in the future.

Acknowledgment. The authors greatly appreciated the frequent discussions with Prof. Keller and Dr. Odell; the financial support from the Swiss National Science Foundation is gratefully acknowledged.

References and Notes

(1) Porter, R. S.; Casale, A. *Polym. Eng. Sci.* **1985**, *25*, 129.
(2) Ballauff, M.; Wolf, B. A. *Adv. Polym. Sci.* **1988**, *85*, 1.
(3) Keller, A.; Odell, J. A. *Colloid Polym. Sci.* **1985**, *263*, 181.
(4) Odell, J. A.; Keller, A. *J. Polym. Sci., Polym. Phys. Ed.* **1986**, *24*, 1889.
(5) Nguyen, T. Q.; Kausch, H. H. *Colloid Polym. Sci.* **1986**, *264*, 764.
(6) Nguyen, T. Q.; Kausch, H. H. *J. Non-Newtonian Fluid Mech.* **1988**, *30*, 125.
(7) Frank, F. C.; Keller, A.; Mackley, M. R. *Polymer* **1971**, *12*, 467.
(8) Zimm, B. H. *J. Chem. Phys.* **1956**, *24*, 269.
(9) Marcucci, G. *Polym. Eng. Sci.* **1975**, *15*, 229.
(10) Merrill, E. W.; Horn, A. F. *Polym. Commun.* **1984**, *25*, 144.
(11) Nguyen, T. Q.; Kausch, H. H. *Chimia* **1986**, *40*, 129.
(12) Sohma, J.; Ishihara, O.; Kobayashi, T. *Rep. Prog. Polym. Phys. Jpn.* **1986**, *29*, 595.
(13) Ederer, H. J.; Basedow, A. M.; Ebert, K. H. *Modelling of Chemical Reaction Systems*; Springer Verlag: Berlin, Heidelberg, 1981; pp 189–215.
(14) Barth, H. G.; Carlin, F. J. Jr. *J. Liq. Chromatogr.* **1984**, *7*, 1717.
(15) Zhurkov, S. N.; Korsukov, V. E. *J. Polym. Sci., Polym. Phys. Ed.* **1974**, *12*, 385.
(16) Bestul, A. B. *J. Chem. Phys.* **1956**, *24*, 1196.
(17) Odell, J. A.; Keller, A.; Rabin, Y. *J. Chem. Phys.* **1988**, *88*, 4022.
(18) Casale, A. *J. Appl. Polym. Sci.* **1975**, *19*, 1461.
(19) Odell, J. A., private communication, 1989.
(20) Merrill, E. W.; Leopairat, P. *Polym. Eng. Sci.* **1980**, *20*, 505.
(21) Rabin, Y.; Wang, S.-Q.; Freed, K. F. *Macromolecules* **1989**, *22*, 2420.
(22) Flory, P. J. *Principles of Polymer Chemistry*; Cornell University Press: Ithaca, NY, 1953.
(23) Elias, H. G.; Bührer, H. G. *Polymer Handbook*, 2nd ed.; Wiley-Interscience: New York, 1975; p IV-57.
(24) Flory, P. J. *Principles of Polymer Chemistry*; Cornell University Press: Ithaca, NY, 1953; p 606.
(25) Nguyen, T. Q.; Kausch, H. H. *Makromol. Chem.* **1989**, *190*, 1389.
(26) POLYFLOW, a finite element program for calculating viscous and viscoelastic flows: Polyflow, S. A., Fonds Jean Paques 8, B-1348 Louvain-la-Neuve, Belgium.
(27) Armstrong, R. C.; Gupta, S. K.; Basaran, O. *Polym. Eng. Sci.* **1980**, *20*, 466.
(28) Nguyen, T. Q.; Kausch, H. H., manuscript in preparation.
(29) Farrell, C. J.; Keller, A.; Miles, M. J.; Pope, D. P. *Polymer* **1980**, *21*, 1292.
(30) Hamielec, A. E. *Steric Exclusion Liquid Chromatography of Polymers*; Marcel Dekker: New York, 1984; pp 117–160.
(31) Nguyen, T. Q.; Kausch, H. H. *J. Chromatogr.* **1988**, *449*, 63.
(32) de Gennes, P.-G. *J. Chem. Phys.* **1974**, *60*, 5030.
(33) Ambari, A.; Deslouis, C.; Tribollet, B. *Phys. Chem. Hydrodyn.* **1985**, *6*, 815.
(34) Pope, D. P.; Keller, A. *Colloid Polym. Sci.* **1978**, *256*, 751.
(35) Wiest, J. M.; Bird, R. B. On Coil-Stretch Transitions in Dilute Polymer Solutions. Rheology Research Center Report, University of Wisconsin: Madison, WI, 1988.
(36) Larson, R. G.; Magda, J. J. *Macromolecules* **1989**, *22*, 3004.
(37) Fuller, G. G.; Leal, L. G. *Rheol. Acta* **1980**, *19*, 580.
(38) Cathey, C. A.; Fuller, G. G. Internal Report, Department of Chemical Engineering, Stanford University, 1988.
(39) Rabin, Y. *J. Chem. Phys.* **1987**, *86*, 5215.
(40) Kausch, H. H. *Polymer Fracture*, 2nd ed.; Springer Verlag: Berlin, Heidelberg, 1987; p 129.
(41) Park, I. H.; Wang, Q.-W.; Chu, B. *Macromolecules* **1987**, *20*, 1965.
(42) Kuhn, W.; Kuhn, H. *Helv. Chim. Acta* **1944**, *27*, 493.
(43) Frenkel, J. *Acta Physicochim. URSS* **1944**, *19*, 51.
(44) Ryskin, G. *J. Fluid Mech.* **1987**, *178*, 423.
(45) Müller, A. J.; Odell, J. A.; Keller, A. *J. Non-Newtonian Fluid Mech.* **1988**, *30*, 99.
(46) Kuhn, W.; Kuhn, H. *Helv. Chim. Acta* **1945**, *28*, 1533; **1946**, *29*, 609, 830.
(47) Cerf, R. *J. Polym. Sci.* **1957**, *23*, 125.
(48) de Gennes, P.-G. *J. Chem. Phys.* **1977**, *66*, 5825.
(49) Winnik, M. A.; Redpath, T.; Richards, D. H. *Macromolecules* **1980**, *13*, 328.

Registry No. Polystyrene, 9003-53-6.